Visual Abstract

Impact behavior of gravity cast AlSi10Mg alloy: Effect of hot isostatic pressing and innovative high pressure T6 heat treatment

Luca Girelli
Department of Mechanical and Industrial Engineering, University of Brescia, via Branze 38, 25123 Brescia, Italy
l.girelli005@unibs.it, http://orcid.org/0000-0002-7630-0662

Maverick Giovagnoli
Department of Engineering, University of Ferrara, via Saragat 1, 44122 Ferrara, Italy
maverick.giovagnoli@unife.it, http://orcid.org/0000-0002-9214-3919

Marialaura Tocci
Department of Mechanical and Industrial Engineering, University of Brescia, via Branze 38, 25123 Brescia, Italy
marialaura.tocci@unibs.it, http://orcid.org/0000-0002-7515-0615

Annalisa Fortini
Department of Engineering, University of Ferrara, via Saragat 1, 44122 Ferrara, Italy
annalisa.fortini@unife.it, http://orcid.org/0000-0002-9774-7105

Marcello Gelfi
Department of Mechanical and Industrial Engineering, University of Brescia, via Branze 38, 25123 Brescia, Italy
marcello.gelfi@unibs.it, http://orcid.org/0000-0002-8939-811X

Mattia Merlin
Department of Engineering, University of Ferrara, via Saragat 1, 44122 Ferrara, Italy
mattia.merlin@unife.it, http://orcid.org/0000-0003-4685-1073

Annalisa Pola
Department of Mechanical and Industrial Engineering, University of Brescia, via Branze 38, 25123 Brescia, Italy
annalisa.pola@unibs.it, http://orcid.org/0000-0002-0722-6518

ABSTRACT. In the present study, the impact behavior of gravity casting AlSi10Mg alloy was evaluated with an instrumented Charpy pendulum. The effect of hot isostatic pressing, also followed by a T6 treatment, was analyzed in comparison with samples in the as-cast, annealed and T6 conditions. Furthermore, the effect of the innovative high-pressure T6 was investigated.

OPEN ACCESS

Citation: Girelli, L., Giovagnoli, M., Tocci, M., Fortini, A., Gelfi, M., Merlin, M., Pola, A., Impact behavior of gravity cast AlSi10Mg alloy: Effect of hot isostatic pressing and innovative high pressure T6 heat treatment,

It was found that the hot isostatic pressing is able to ensure densification of the alloy with an increase in both hardness and energy absorbed during impact. The T6 treatment performed at atmospheric pressure after the hot isostatic pressing is able to increase hardness and peak force. At the same time, the innovative high-pressure T6 is able to ensure similar results than those of hot isostatic pressing followed by T6, leading to a significant decrease in the treatment duration and costs and reducing the carbon footprint of the manufacturing process.

KEYWORDS. AlSi10Mg, Hot isostatic pressing, High pressure heat treatment, Impact, Fracture surface.

Frattura ed Integrità Strutturale, 64 (2023) 204-217.

Received: 22.12.2022
Accepted: 28.02.2023
Online first: 01.03.2023
Published: 01.04.2023

INTRODUCTION

Aluminum alloys are widely used metallic materials, thanks to their high strenght-to-mass ratio, especially for the lightweighting in the automotive industry, where the reduction of both energy consumption and CO_2 emissions is a continuously increasing demand. At the same time, these alloys have been introduced in the production of commercial vehicles and trucks also to allow additional transportation load as a result of a weight reduction of the vehicle itself.

Moreover, it is known that aluminum alloys can be continuously recycled, further representing an optimal choice to reduce the carbon footprint of the automotive sector. In fact, the life cycle assessment of a vehicle considers not only the fuel (or electric energy) consumption for the movement, but also the total emissions related to the production of each component, from the raw material to the assembling line.

Among the families of aluminum alloys, the Al-Si-Mg ones represent the most used for the production of cast parts, such as wheels, engines, brake calipers, pistons, gearboxes, etc. This is due to their excellent properties in terms of castability and limited thermal expansion (thanks to the presence of silicon) and, at the same time, in terms of good mechanical properties. The presence of Mg ensures the precipitation of Mg_2Si compounds that are able to guarantee a significant increase in mechanical properties after precipitation hardening heat treatment. For this reason, Al-Si-Mg alloys are widely used to produce automotive structural components by gravity casting.

Another treatment that can be carried out on this material to reduce residual stresses related to the manufacturing process is the annealing.

Unfortunately, foundry processes, such as gravity casting, usually leave some porosities in the casting that can affect mechanical properties. In fact, casting defects as shrinkage pores and oxide films are known to be the initiation sites for fracture [1], resulting in a reduction of the mechanical properties of the alloy.

With the aim of reducing the internal pores (gas pores and interdendritic shrinkage), hot isostatic pressing (HIP) is nowadays conventionally used for additive manufacturing products [2-4], and its use has also been proposed on castings [5-7]. The HIP consists in a heat treatment under high pressure during which the porosities are progressively closed and sealed, ensuring metallurgical integrity. HIP is usually followed by the conventional T6 treatment to reach the required mechanical properties.

Several studies have documented the effective densification of castings after HIP and the consequent effect on the performance of Al-Si alloys. Ceschini et al. [8], for example, analyzed the effect of HIP on an AlSi10Cu2 with different Fe contect finding that the HIP only induced a slight increase on the fatigue resistance due to the presence of β-Al5FeSi intermetallics compared to the alloy without Fe. Ran et al. [9] found that HIP reduced the porosity volume fraction and pore size of an A356 alloy, improving its ductility, but it was not able to produce a significative improvement in tensile strength because of the brittle unmodified microstructure. Lee et al. [10], analyzing the fatigue resistance of an A356 alloy, showed that hot isostatic pressing was able to increase fatigue strength as a consequence of the reduction of porosity volume fraction, with an initiation of the cracks at eutectic Si particles rather than at pores close to the surface as for the not hipped samples.

Lately, a different route has been tested, combining HIP and T6 in a single treatment carried out under pressure in the same HIP vessel. In this case, the HIP is used as a solution treatment, then the castings are quenched using pressurized cold gas, and subsequently the temperature is increased to the aging temperature, still applying a relevant pressure and without removing the castings from the vessel. In this way, it is possible to achieve the densification ensured by the HIP treatment and the hardening due to the formation of strengthening precipitates during the aging treatment in a time-effective way.

Hafenstein et al. [11] studied this treatment for sand AlSi7Mg castings and found that a quenching rate of 6.9 °C/s inside the pressurized vessel, in the temperature range between 540 °C and 200 °C, is enough to achieve a suitable oversaturated solid solution and, therefore, the aging can be directly carried out after hot isostatic pressing. This means that no other step of solution treatment is necessary, reducing the treatment duration and costs. The key role of the quenching under pressure is demonstrated by another work by Hefenstein et al. [12], where they performed tensile tests and Rumul high frequency fatigue tests on AlSi7Mg0.3 alloy undergoing conventional hot isostatic pressing, followed by aging at ambient pressure. In this case, HIP replaced the solution treatment. The fatigue resistance and the elongation were found to be increased by the traditional HIP (i.e. without subsequent solution annealing but followed by aging), while hardness and ultimate tensile strength were lower than those of the as-cast alloys. The authors attributed this result to the slow cooling rate (0.2 °C/s) of the conventional HIP, which brings stable and coarse precipitates of Si and Mg at elevated temperatures. For this reason, not enough Si and Mg atoms in solid solution can form needle-like β" precipitates during aging, leading to an insufficient strengthening of the alloy. The high pressure T6, allowing higher cooling rates, overcome this issue. In fact, the effectiveness of the high pressure T6 heat treatment was studied on AlSi7Mg alloy produced by casting or on the AlSi10Mg alloy produced by additive manufacturing [13-14].

At the same time, the effect of this treatment on gravity casting AlSi10Mg alloys is not likewise analyzed, especially considering the influence of the heat treatment on impact behavior. However, it could represent an appropriate choice for enhancing material performance and, therefore, promoting the lightweighting of components.

In the present study, the impact behavior of the AlSi10Mg alloy, also known as EN AC 43200, manufactured by gravity casting is investigated after various heat treatment routes. In detail, the effect of hot isostatic pressing without any other treatment (HIP), hot isostatic pressing followed by the traditional T6 (HIP+T6) and the high pressure T6 treatment (HPT6), was evaluated. In parallel, the analysis was performed on the alloy in the as-cast condition, after the conventional annealing and after the traditional T6 treatment.

Experimental procedure

The AlSi10Mg samples for the impact test were taken from an automotive structural component produced through gravity casting in a steel permanent mold. The alloy was previously melted in a gas furnace and degassed with nitrogen. Na was added for Si modification and Ti-B for grain refinement.

The chemical composition of the alloy was measured by means of an optical emission spectrometer, and it is reported in Tab. 1.

Si	Mg	Fe	Mn	Cu	Ti	Na	Al
9.89 ± 0.30	0.376 ± 0.037	0.508 ± 0.021	0.403 ± 0.019	0.207 ± 0.011	0.091 ± 0.006	0.066 ± 0.002	balance

Table 1: Chemical composition (wt. %) of the gravity cast AlSi10Mg alloy.

At first, cylinders with a diameter of approximately 20 mm and a length of approximately 60 mm were machined from areas of the casting with the same thickness to ensure similar microstructure due to similar cooling rates and solidification conditions.

The samples were subjected to three different combinations of hot isostatic pressing and heat treatments:

- Hot isostatic pressing at 520 °C for 2 hours without any other additional treatment (HIP).
- Hot isostatic pressing at 520 °C for 2 hours followed by a traditional T6 heat treatment (T6) not under pressure (HIP+T6). The T6 treatment consisted of solution treatment at 520 °C for 2 hours, quenching in water at 65 °C, and aging at 180 °C for 4 hours at atmospheric pressure.
- Hot isostatic pressing at 520 °C for 2 hours followed by quenching and aging at 180 °C for 4 hours under pressure. This is the innovative under pressure T6 heat treatment (HPT6).

For each combination of hot isostatic pressing and heat treatment (HIP, HIP+T6, HPT6), whose temperature scheme is reported in Fig. 1, two different values of pressure were selected: 50 MPa, and 150 MPa. The subscripts 50 and 150 hereinafter refer to 50 MPa and 150 MPa, respectively.

Normally, during hot isostatic pressing, the vessel is filled with an inert gas (e.g., Ar), which acts as an intermediate medium to apply pressure to the components. The use of gas ensures the application of an isostatic pressure since the gas can reach

all the surfaces of the components, regardless of shape, and the applied pressure is the same for every surface and it acts along the direction normal to the surface.
To evaluate the effectiveness of the hot isostatic pressing, the characterization was performed for comparison on samples in as-cast (AC), annealed (AN) and traditional T6 conditions (T6).
The annealing heat treatment was performed at 300 °C for 2 hours at atmospheric pressure and it was followed by air cooling. Instead, the traditional T6 heat treatment was conducted with a solution at 520 °C for 2 h, quenching in water at 65 °C, and aging at 180 °C for 4 hours at atmospheric pressure.
The density was calculated through Eqn. (1) ($m_{sample\ in\ air}$ is the mass of the sample in air, $m_{sample\ in\ water}$ is the mass of the sample in water, and ρ_{water} is the water density equal to 1.0 g/cm^3) using a Mettler AE240 weight scale and measuring the mass of at least two specimens for each test condition in both air and distilled water, according to the Archimedes hydrostatic weighing method.

$$\rho_{sample} = \rho_{water} \cdot \frac{m_{sample\ in\ air}}{m_{sample\ in\ air} - m_{sample\ in\ water}} \tag{1}$$

The results obtained by the hydrostatic method were compared with those from microstructural image analysis for each tested condition.

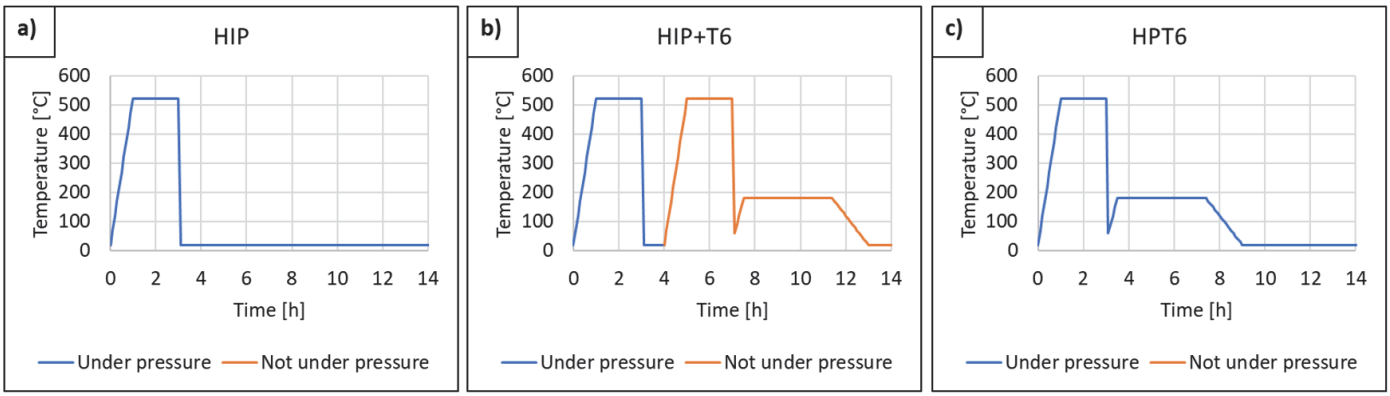

Figure 1: Temperature-time correlation for the 3 different types of treatment: (a) hot isostatic pressing (HIP); (b) hot isostatic pressing and T6 heat treatment at atmospheric pressure (HIP+T6); (c) innovative under pressure T6 heat treatment (HPT6).

After the treatments (for the as-cast condition without performing any heat treatment), the Charpy impact specimens (55 mm x 10 mm x 10 mm) with a U-notch were machined according to ASTM E23 standard from the cylinders.
The microstructural analysis was performed using a Leica DMi8A (Leica, Wetzlar, Germany) optical microscope. A section of the specimens perpendicular to the impact direction was observed. In detail, the samples were cut with metallographic cutting machine with a SiC cut-off wheel, mounted in epoxy resin, and manually grinded on SiC abrasive papers (mesh of P320, P600, P800, and P1200) using tap water as lubricant. Subsequently, the samples were manually polished up to mirror-like finishing on polishing clothes, using water-based lubricant in combination with 3 μm and, subsequently, 1 μm diamond suspensions and, finally, using oxide polishing with OP-S 0.25 μm. The polishing duration was at least 1 minute for each of abrasive paper and at least 5 minutes for each (3 μm and 1 μm) diamond suspension. The metallographic analysis was performed without any chemical etching.
The results obtained by the hydrostatic method were compared with those from microstructural image analysis. This analysis was carried out by means of the ImageJ software, coupled to the Leica DMi8A (Leica, Wetzlar, Germany) optical microscope, on 25 micrographs collected from the as-polished samples for each test condition. Image analysis was performed on each binarized image and porosity was computed as the ratio of pores area to the total area of the image. The analysis was carried out for as-cast, annealed and T6-treated samples to evaluate the effect of low- and high-temperature treatment at atmospheric pressure on both the size and distribution of Si particles. The image analysis was not carried out on the samples treated under pressure since it has been already demonstrated that for an AlSi10Mg alloy produced by laser powder bed fusion a pressure of 150 MPa is not able to significantly affect the size and distribution of Si particles, while the time and temperature have a major influence on diffusion phenomena than this range of pressure [13]. Therefore, it can be

assumed that T6, HIP and HPT6 treatments have the same effect on the size and distribution of Si particles since the time and temperature of the solution/HIP step are the same.
The mirror-like polished surface of AlSi10Mg samples in as-cast condition was also analysed by energy dispersive X-ray spectroscopy (EDX) to investigate Fe-intermetallic compounds.
The hardness was measured on the polished samples using the Brinell method according to ASTM E10 standard with a LTF Galileo Ergotest Comp25 apparatus applying a load of 613 N for a dwell time of 15 s and using a tungsten carbide ball of 2.5 mm in diameter as indenter.
The Charpy impact tests were performed at room temperature with a Ceast instrumented pendulum with 50 J of available energy. The data were acquired with a Das 64k analyzer and elaborated with Matlab® code according to the ISO 14556:2015 standard about force-displacement curves. At least three repetitions were carried out for each condition.
After the impact tests, the observation of fracture surfaces was carried out using a Zeiss Evo MA 15 (Zeiss, Oberkochen, Germany) scanning electron microscope, while the observation of fracture profiles was performed by the Leica DMi8A optical microscope on resin mounted samples polished to mirror-like finishing.

Results and discussion

Microstructure, density, and hardness

The microstructure of the AlSi10Mg alloy (Fig. 2) is composed of the α-Al dendrites, the eutectic phase and the Fe-intermetallics. In the as-cast (Fig. 2.a), annealed (Fig. 2.b) and T6 (Fig. 2.c) conditions, a significant presence of porosity can be detected, while the only HIP (Fig. 2.d,g) ensures a strong reduction in porosity. As an example, a-Al dentrites, eutectic phase and porosity are clearly indicated in Fig. 2.a.
The other treatments that involve the application of pressure, as HIP+T6 (Fig. 2.e,h) and HPT6 (Fig. 2.f,i), appear to maintain the low porosity level observed for the only HIP condition.

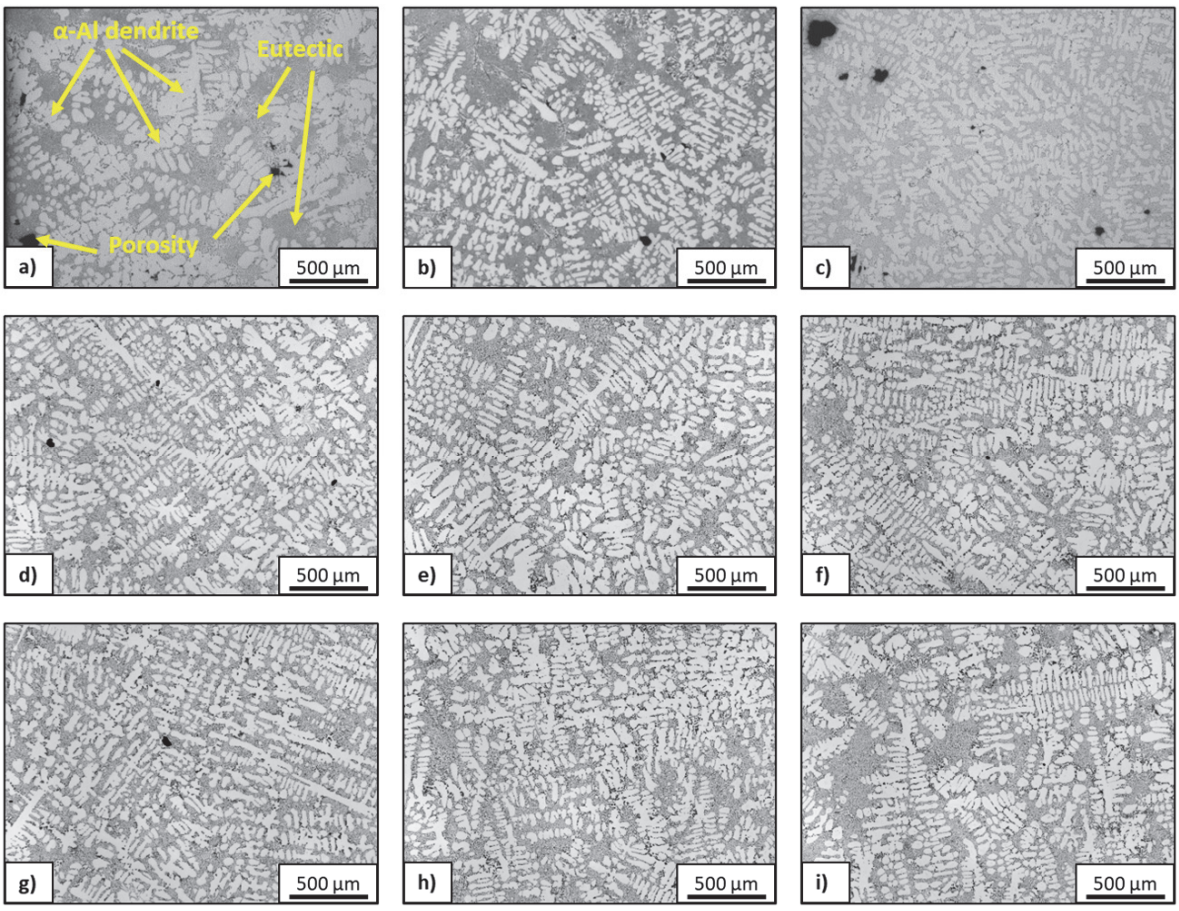

Figure 2: Microstructure of gravity cast samples in (a) as-cast, (b) annealed, (c) T6, (d) HIP_{50}, (e) HIP_{50}+T6, (f) $HPT6_{50}$, (g) HIP_{150}, (h) HIP_{150}+T6, (i) $HPT6_{150}$ conditions.

On the as-cast polished specimens, the energy dispersive X-ray (SEM-EDX) analysis shows the presence of various morphologies of Fe-bearing intermetallics, such as α-Fe, β-Fe, π-Fe, and Q-phases, as reported in Fig. 3. This is due to the presence of relevant content of Fe, together with other alloying elements as Mn and Cu, that are known to easily combine with Fe and form complex intermetallic particles. In particular, β-Fe (Fig. 3.c, 3.h) is the most common intermetallic compound in foundry alloys and it is characterized by a plate-like morphology. Therefore, it appears as needle-like when observing a cross-section under a microscope. The α-Fe (Fig. 3.a-b, 3.g) is characterized by a blocky morphology, associated to the presence of Mn, while π-Fe (Fig. 3.e, 3.i), containing Mg, exhibits a Chinese script one [15]. Intermetallic compounds containing Cu were also detected (Fig. 3.f, 3.j). These particles are generally not significantly affected by heat treatments such as those considered in the present study. It is well known that intermetallic particles are brittle compounds, which therefore reduce the ductility and the toughness of the alloy according to their size and number. Finally, some Mg_2Si compounds are visible (Fig. 3.d).

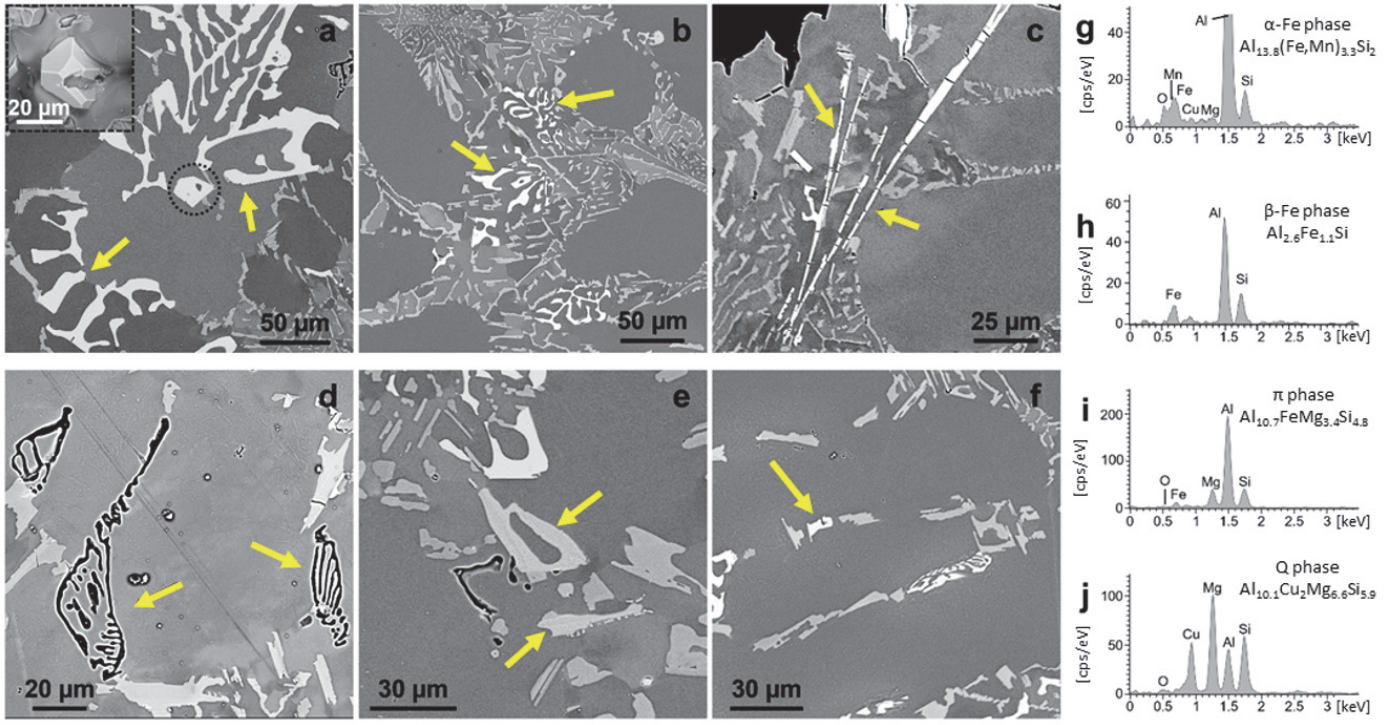

Figure 3: The intermetallic phases of the as-cast material observed through scanning electron microscopy with the energy dispersive X-ray analysis. The arrows indicate the intermetallics subjected to analysis.

The image analysis performed after the heat treatments at atmospheric pressure shows that annealing (Fig. 4.b) and T6 (Fig. 4.c) treatments lead to fragmentation and spheroidization of the eutectic Si in comparison with the as-cast condition (Fig. 4.a), as expected [16].

After annealing, the Si particles appear slightly smaller in size as reported in the Probability Density Function (PDF) plot for the Equivalent Diameter (Fig. 4.d), but still elongated, as indicated by the distribution in terms of aspect ratio (Fig. 4.e). After the T6 heat treatment (Fig. 4.c), the statistical distribution of the eutectic Si equivalent diameter values (Fig. 4.d) shows an increase of the peak of approximately 20 % in comparison with the as-cast sample (Fig. 4.a), indicating a higher number of particles with an equivalent diameter of 1-2 µm than under the other conditions. This result suggests that the Si particles are more homogeneous in size, while Fig. 4.e shows that these particles are also more rounded due to the spheroidization.

The relative density, calculated by both Archimedes' hydrostatic weighing method and image analysis, was presented in Fig. 5, assuming as 100 % the density of the specimen with the highest measured value.

The image analysis performed for the as-cast condition shows an average density of 98.5 % in perfect agreement with the result obtained by the weighing method. On the other hand, a significant scattering of the results from image analysis is evident, due to the variation of the size and distribution of the pores in the micrographs.

The annealing and the T6 heat treatment do not lead to a significant variation in density from the as-cast condition.

After hot isostatic pressing without further treatment (HIP_{50} and HIP_{150}), the relative density reaches approximately 100 % according to both testing methods. After an additional heat treatment (HIP_{50}+T6 and HIP_{150}+T6, $HPT6_{50}$ and $HPT6_{150}$),

the data obtained from image analysis confirm the full density of the samples, while those from weighing methods are slightly lower (99.5 %), but still close to the full density as a possible consequence of an expansion of the alloy after ageing [17]. In general, an increase of about 1 % compared to the as-cast condition is measured.

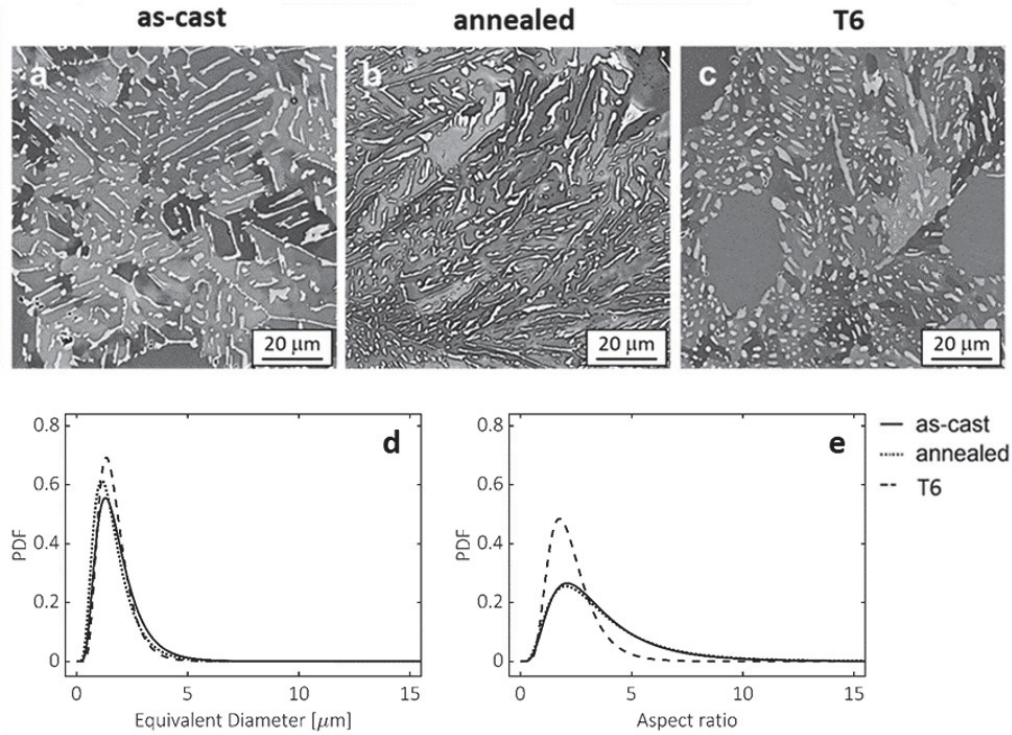

Figure 4: Effect of heat treatment at atmospheric pressure on the eutectic Si: (a) as-cast condition, (b) annealed condition, (c) T6 conditions, (d) distribution of the values of particles' equivalent diameter, (e) distribution of the values of the particles' aspect ratio.

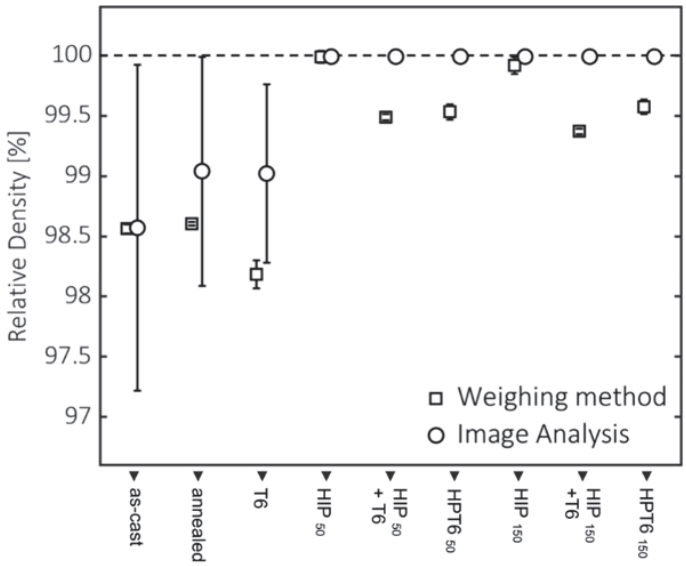

Figure 5: Comparison chart between weighing method and image analysis about density measurements.

The hardness results are reported in Tab. 2.

After the annealing treatment, an increase in hardness of less than 10 % can be observed as a possible consequence of a partial spheroidization of Si particles. After the T6 heat treatment, an average increase in hardness of about 60 % can be measured as an effect of the spheroidization of Si particles and especially on the precipitation of Mg_2Si compounds.

After HIP alone at both 50 and 150 MPa (HIP_{50} and HIP_{150}), an increase in hardness of about 37 % is obtained, as shown in Tab. 2. The increase in hardness could be related to multiple factors. As a result of the soaking at high temperature for

2 hours, the reduction of porosity, as a consequence of plastic deformation in the castings and collapse of the defect [5], is definitely positive for the hardness of the material, together with the fragmentation and spheroidization of the Si particles. The small size and rounded shape make Si particles more effective at withstanding the load and hindering displacement movement [18-19]. Finally, after HIP the samples are hardened and the consequent hardening of the Al matrix due to the strengthening of the solid solution and natural aging can further contribute to the increase in hardness compared to the as-cast condition.
A further increase in hardness is achieved after HIP followed by T6 (HIP_{50}+T6 and HIP_{150}+T6) and after T6 treatments under pressure ($HPT6_{50}$ and $HPT6_{150}$).
After the only HIP at both 50 and 150 MPa (HIP_{50} and HIP_{150}), an increase in hardness of about 37 % is obtained, as indicated in Tab. 2. The increase in hardness could be correlated to multiple factors. As a result of the soaking at high temperature for 2 hours, the reduction of porosity, as a consequence of plastic deformation in castings and the defect collapsing [5], is surely positive for material hardness, together with the Si particles fragmentation and spheroidization. The smaller size and the rounded shape make the Si particles more effective in bearing the load and hindering the dislocation movement [18-19]. Finally, after HIP the samples are quenched and the consequent hardening of the Al matrix due to solid solution strengthening and natural aging can further contribute to the increase in hardness as compared to the as-cast condition.
A further increase in hardness is obtained after HIP followed by T6 (HIP_{50}+T6 and HIP_{150}+T6) and after T6 treatments under pressure ($HPT6_{50}$ and $HPT6_{150}$).
The biggest increase is observed with the combination of HIP at 150 MPa and the T6 treatment under atmospheric pressure (HIP_{150}+T6), where the hardness rises the value of 112 HB (+ 78 % in comparison with the as-cast condition). Nevertheless, the results obtained with other conditions (HIP_{50}+T6, $HPT6_{50}$, $HPT6_{150}$) are very similar.

	AC	AN	T6	HIP_{50}	HIP_{50}+T6	$HPT6_{50}$	HIP_{150}	HIP_{150}+T6	$HPT6_{150}$
Hardness (HBW)	63 ± 2	68 ± 2	100 ± 2	86 ± 3	110 ± 2	108 ± 2	87 ± 2	112 ± 1	107 ±3
Variation from AC condition (%)	-	+ 8 %	+ 59 %	+ 37 %	+ 75 %	+ 71 %	+ 38 %	+ 78 %	+ 70 %

Table 2: Results of Brinell hardness tests (HBW) for the tested conditions with the percentage variation compared to the as-cast condition.

Considering density and hardness results, the innovative heat treatment under pressure (HPT6) ensures similar results to that obtained after HIP+T6 treatment, reaching almost full density and hardness values above 105 HB, but in a shorter time. In fact, the HPT6 route leads to a treatment time saving of about 4 hours. This reduction of the treatment duration means a decrease of energy consumption and, therefore, of CO_2 emissions in the atmosphere, contributing to reducing the carbon footprint of the heat treated AlSi10Mg gravity cast component.
At the same time, an increase in pressure treatment from 50 MPa to 150 MPa is not able to ensure better results in terms of density and hardness for both HPT6 and HIP+T6 routes.

Impact tests

Regarding the response of the specimens to the Charpy impact test, a representative force-displacement curve is reported in Fig. 6 as an example for each tested condition. The initiation energy, which corresponds to the energy absorbed by the sample until the force reaches the highest value (peak force), is identified with blue color, while the propagation energy is identified with green color. The peak displacement is the displacement corresponding to the peak force, which is the highest value of the force measured by the instrumented pendulum.
All the results from impact tests are reported in Tab. 3.
The as-cast AlSi10Mg sample (Fig. 6.a) shows a peak force of 2.9 ± 0.2 kN with an initiation energy of 0.8 ±0.1 J and a propagation energy of 1.1 ± 0.1 J (Tab. 3). This result could be associated with the presence of porosity (Fig. 2.a) and of coarse and elongated particles of Si (Fig. 4.a).
After the annealing (Fig. 6.b), no appreciable variations can be observed with respect to the as-cast condition, leading to the conclusion that, from the impact point of view, this treatment is not able to modify the behavior of the alloy even though a first fragmentation and spheroidization of Si particles has occurred, as observed from microstructures (Fig. 2.b and Fig. 4.b).

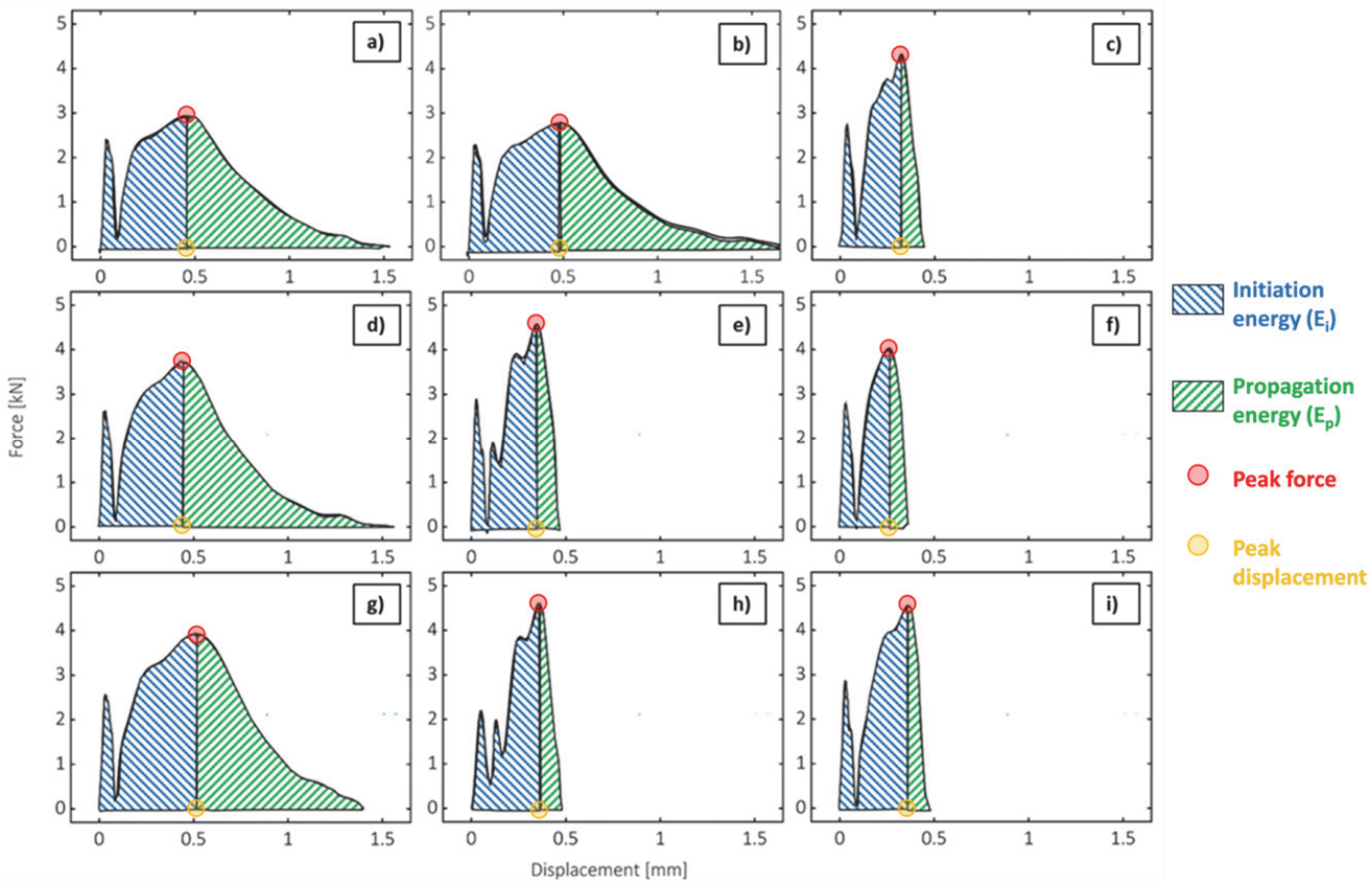

Figure 6: A single force-displacement curve for gravity cast specimen in (a) as-cast, (b) annealed, (c) T6, (d) HIP_{50}, (e) HIP_{50}+T6, (f) $HPT6_{50}$, (g) HIP_{150}, (h) HIP_{150}+T6, (i) $HPT6_{150}$ conditions.

	AC	AN	T6	HIP_{50}	HIP_{50}+T6	$HPT6_{50}$	HIP_{150}	HIP_{150}+T6	$HPT6_{150}$
Fp [kN]	2.9 ± 0.2	2.6 ± 0.2	3.9 ± 0.6	4.0 ± 0.4	4.7 ± 0.2	4.6 ± 0.8	3.9 ± 0.1	4.3 ± 0.2	4.6 ± 0.1
Ei [J]	0.8 ± 0.1	0.9 ± 0.1	0.6 ± 0.3	1.5 ± 0.5	0.9 ± 0.1	0.8 ± 0.3	1.3 ± 0.1	0.8 ± 0.1	0.9 ± 0.1
Ep [J]	1.1 ± 0.1	1.1 ± 0.1	0.4 ± 0.1	1.5 ± 0.4	0.3 ± 0.1	0.3 ± 0.1	1.4 ± 0.1	0.3 ± 0.1	0.3 ± 0.1

Table 3: Force-displacement results of all the tested specimens, where *Fp* is the peak force, *Ei* is the initiation energy, and *Ep* is the propagation energy.

Instead, after the T6 heat treatment (Fig. 6.c), a very important reduction in propagation energy (from 1.1 ± 0.1 kN to 0.4 ± 0.1 J) can be observed and, at the same time, an increment in peak force (from 2.9 ± 0.2 kN to 3.9 ± 0.6 kN) can be noticed (Tab. 3). This result could be due to the precipitation of Mg_2Si compounds, which strengthen the Al matrix and increases the yield strength of the material, leading to a higher peak force than the as-cast condition, and to the presence of porosities (Fig. 2.c), which reduce the load bearing area and therefore are negative in terms of propagation energy. After T6, the spheroidization of Si particles (Fig. 4.c), which should improve the toughness of the alloy [19], is likely not enough to counteract the negative influence of the presence of porosities that increases from the as-cast condition as demonstrated by a little decrement of the density measured by the weighing method (Fig. 4). The consequence is that the initiation energy is very similar for both AC and T6 conditions. During impact tests, porosities, together with intermetallics and coarse Si particles, easily play the role of stress concentrators, reducing the initiation energy for both AC and T6 samples.
The only HIP treatment performed at both 50 MPa (Fig. 6.d) and 150 MPa (Fig. 6.g) determines an increase of the peak force, that reaches value of approx. 4 kN, while the values of initiation and propagation energy are 50 % higher than those of as-cast condition (Tab. 3). This result could be correlated at first with the closure of the porosities, and the consequent increase in load bearing area, but also with a spheroidization of Si particles after soaking at 520 °C for 2 hours, which

provides a positive contribution in terms of energy propagation. On the other hand, since no aging was performed, the ductility of the alloy is maintained, further contributing to a high energy absorption.
The T6 heat treatment carried out after hot isostatic pressing (HIP+T6) performed at both 50 MPa (Fig. 6.e) and 150 MPa (Fig. 6.h) leads to a further increment of the peak force (that reaches about 4.5 kN), but at the same time produces a decrease of the initiation energy to values similar to those of as-cast and T6 conditions and a significant loss in the propagation energy to 0.3 ± 0.1 J (Tab. 3). As compared to the only HIP condition, the strengthening effect provided by the aging treatment determines a lower energy absorption during the impact test and, on the other hand, a high peak force.
The innovative high-pressure T6 treatment (HPT6) at both 50 MPa (Fig. 6.f) and 150 MPa (Fig. 6.i) shows values close to those measured after HIP+T6.
The reduction of both initiation and propagation energy and the increment in peak force after T6, HIP+T6, and HPT6 could be due to the precipitation of Mg_2Si particles [20].
The innovative HPT6 ensures high impact properties and, at the same time, a high value of hardness and almost full density with an important reduction of treatment duration in comparison with the combination of hot isostatic pressing and T6 (HIP+T6)
Considering that no appreciable variation of results can be noticed between the HPT6 performed at 50 MPa and at 150 MPa, the treatment at low pressure ($HPT6_{50}$) represents the best choice of parameters from an energy consumption point of view.
In conclusion, the innovative high pressure T6 (HPT6) heat treatment represents an appropriate treatment for structural components in AlSi10Mg alloy produced through gravity casting.

Fracture surfaces

To better understand the results from impact tests, a further analysis was carried out on the specimens in the as-cast (Fig. 7), T6 (Fig. 8), HIP_{50} (Fig. 9), HIP_{50}+T6 (Fig. 10), and $HPT6_{50}$ (Fig. 11). In detail, the microstructure at high magnification analysed by optical microscope is correlated with fracture surface observed under scanning electron microscope (SEM).

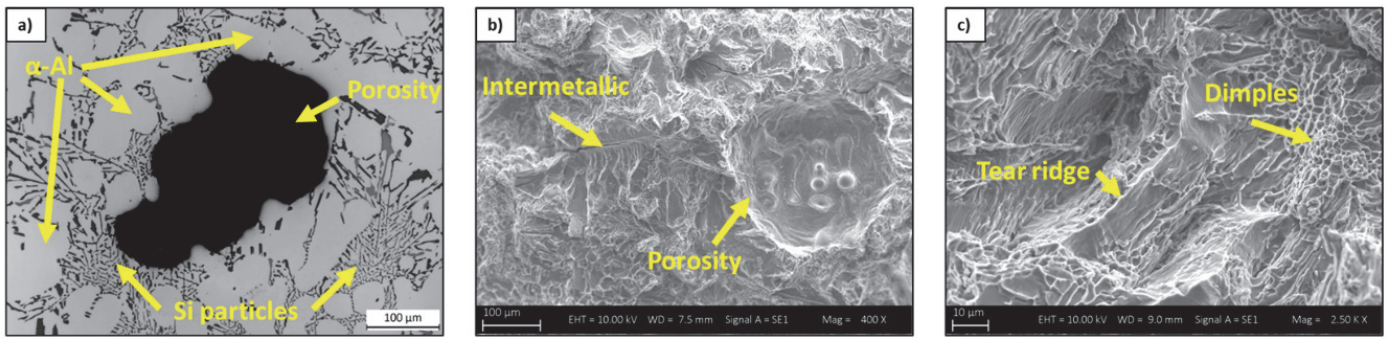

Figure 7: As-cast specimen: (a) microstructure at high magnification by optical microscopy; (b-c) fracture surface by scanning electron microscopy.

The fracture surface (Fig. 7.b-c) of the as-cast specimen shows indications of a ductile behaviour due to the presence of dimples (Fig. 7.c) and, at the same time, cleavage of Si particles.
The presence of porosities and coarse and elongated Si particles in the AC specimen (Fig. 7.a) directly influences the fracture mechanism. In fact, porosities are clearly visible on the fracture surface (Fig. 7.b) of the as-cast specimen, while the presence of flat surfaces likely indicates the cleavage of Si particles of rather coarse size. It can be assumed that the presence of porosities not only reduces the peak force, since it diminishes the load bearing area, but represents an easy path for the fracture to propagate.
Images at higher magnification (Fig. 7.c) also show the presence of dimples, which are signs of a ductile behaviour of the Al matrix, together with tear ridges. These microstructural features indicate a plastic deformation of the matrix, confirmed by the presence of plastic micro-deformation and parallel slip bands visible on the shear surface [21]. In fact, in the as-cast condition, the matrix is not strengthened by precipitates and maintains its ductility. Cracked intermetallic particles are also present (Fig. 7.b).
The T6 heat treated specimen, which is characterized by porosities and finer Si particles (Fig. 8.a), shows a fracture surface (Fig. 8.b) where numerous pores are visible. As for the previous condition, the fracture is likely to propagate connecting close porosities. Furthermore, the large flat surface above the central pore (Fig. 8.b) was revealed from back scattered imaging to be a cracked intermetallic particle.

The cleavage of Si particles (Fig. 8.c) is still present, but the corresponding cleavage areas are smaller in size (as compared to as-cast condition) due to the finer dimensions of the Si particles after T6 treatment. In Fig. 8.c, several cracked Si particles are also visible. It appears that, in this case, the fracture propagates mainly along the eutectic fine Si particles, besides porosities and coarse intermetallics. This mechanism is prevalent in the ductile behaviour of the matrix, which is more brittle in comparison with the as-cast condition because of the precipitation of Mg_2Si compounds. This can explain the low energy propagation measured for the T6 samples as compared to the as-cast ones. On the other hand, the increased strength of the alloy is responsible for the higher peak energy.

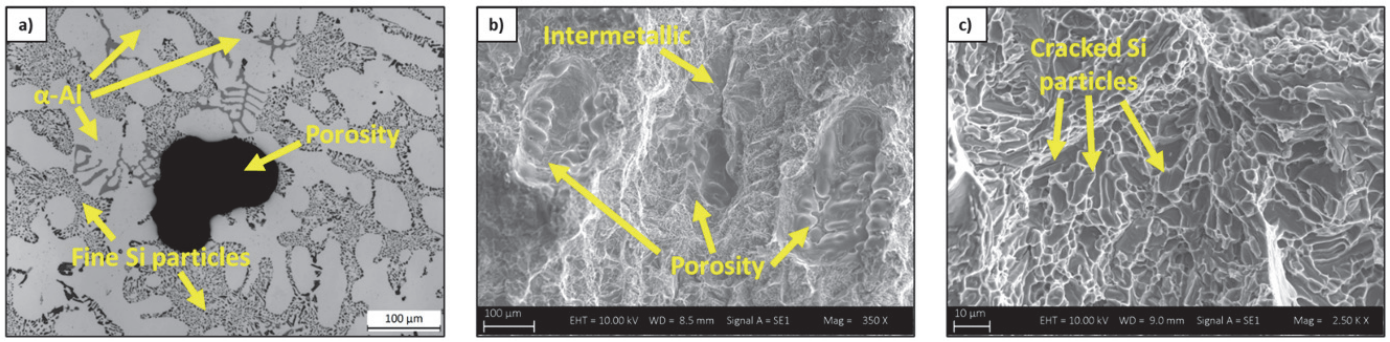

Figure 8: T6 heat treated specimen: (a) microstructure at high magnification by optical microscopy; (b-c) fracture surface by scanning electron microscopy.

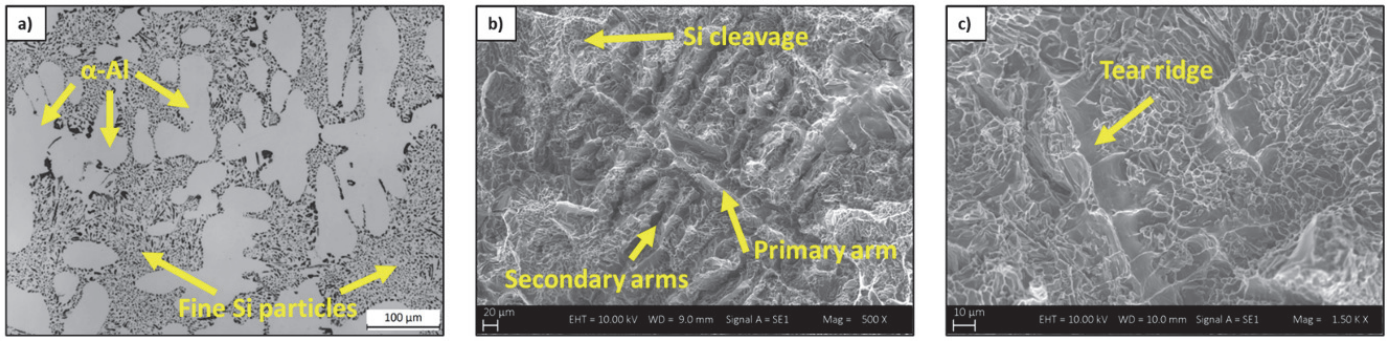

Figure 9: HIP_{50} treated specimen: (a) microstructure at high magnification by optical microscopy; (b-c) fracture surface by scanning electron microscopy.

The HIP_{50} treated specimen is characterized by near-zero porosity (Fig. 9.a) and fine eutectic Si particles that surround the Al dendrites. The presence of intermetallics is not altered by the heat treatment. Consequently, the observation of the corresponding fracture surface (Fig. 9.b) reveals the cleavage of fine Si particles, combined with the prevalent ductile behaviour of the Al matrix that can be assessed due to the presence of dimples.

As mentioned for the as cast sample, tear ridges are visible (Fig. 9.b-c). In Fig. 9.b, it is possible to recognize the shape of primary and secondary arms of a coarse dendrite, while Fig. 9.c shows the detail of a tear ridge. This indicates a plastic deformation of the matrix, confirmed by the presence of plastic micro deformation and parallel slip bands visible on the shear surface [21]. This is consistent with the fact that only HIP does not strengthen the matrix as much as after T6 treatment, which therefore still retains some of the initial ductility, and with the absorbed energy recorded during impact tests.

The HIP_{50}+T6 treated sample is characterized by near-full density and fine eutectic Si particles around the Al dendrites (Fig. 10.a), as for the only HIP_{50} condition (Fig. 9.a). The fracture propagation mainly follows the eutectic Si, revealing a surface fracture with markings of cleavage and cracking of these brittle particles (Fig. 10.b), together with cracked or detached intermetallic particles (Fig. 10.c in back scattered mode). These likely behave as stress concentrators, instead of porosities, which are less abundant after HIP. This can explain the higher E_i as compared to the T6 condition, together with the hardening of the matrix because of the precipitation of Mg_2Si compounds after the T6 heat treatment. This can also be correlated with the higher peak force (Fig. 6.e) than those of only HIP_{50} treated sample (Fig. 6.d). Once the crack is formed, it propagates easily along brittle particles and, in this case, the absence of porosities, is less significant leading to similar propagation energies to the T6 condition.

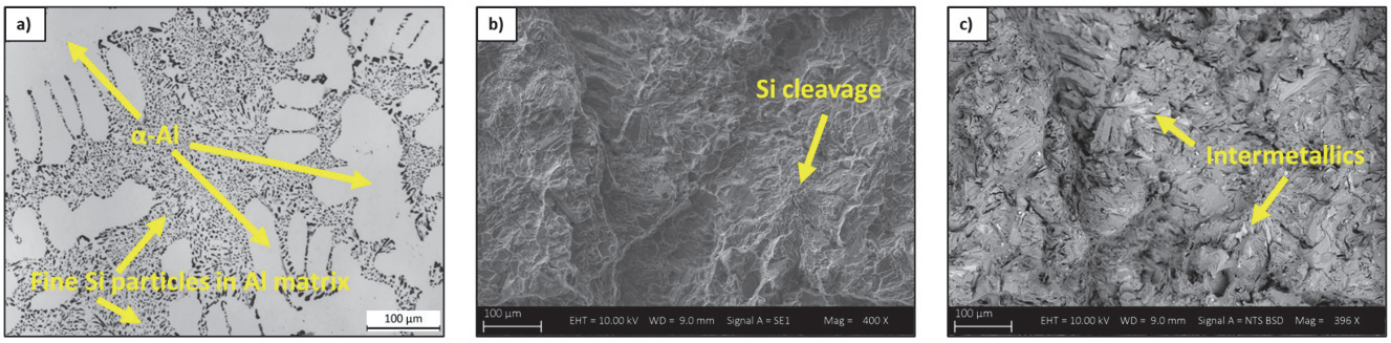

Figure 10: HIP_{50}+T6 treated specimen: (a) microstructure at high magnification by optical microscopy; (b-c) fracture surface by scanning electron microscopy.

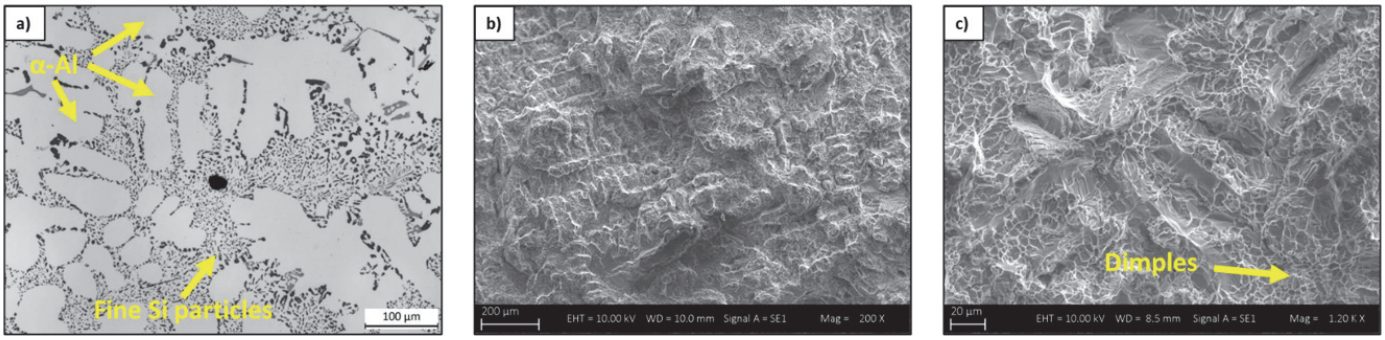

Figure 11: $HPT6_{50}$ treated specimen: (a) microstructure at high magnification by optical microscopy; (b-c) fracture surface by scanning electron microscopy.

The $HPT6_{50}$ treated specimen (Fig. 11.a) shows a low porosity and the same microstructural features already discussed for HIP_{50} (Fig. 9.a) and HIP_{50}+T6 (Fig. 10.a) conditions. As for the HIP_{50}+T6 sample (Fig. 10.b), the fracture initiates and propagates mainly along the Si particles and other brittle compounds (Fig. 11.b). The matrix has a ductile behavior as can be seen by the presence of dimples (Fig. 11.c). The absence of porosities contributes to an increase in the initiation energy, compared to the T6 condition. At the same time, the high peak force could be explained with the precipitation of Mg_2Si compounds during the under pressure T6 as for both the T6 and the HIP+T6 conditions.

Conclusions

This study investigated the impact behavior of a gravity cast AlSi10Mg alloy under multiple treatment conditions. In detail, HIP, HIP+T6 and an innovative HPT6 treatments were carried out. For these treatments, the pressure was set at two different values (i.e. 50 and 150 MPa) to evaluate the influence of this parameter on the final performance. As a comparison with traditional industrial routes, the investigation was also performed on the same alloy under as-cast, annealed and T6 conditions.

The HPT6 treatment resulted in an effective densification and strengthening of the alloy, which reached an almost full density and hardness values above 105 HBW. This was documented also for HIP+T6 samples, but this route requires a longer time. In fact, the HPT6 route led to a treatment time saving of about 4 hours. This reduction of the treatment duration means a decrease in the energy consumption and, therefore, of CO_2 emissions in the atmosphere. This is a positive contribution to the reduction of the carbon footprint for the manufacturing of heat-treated AlSi10Mg gravity cast components. Furthermore, it was found that an increase in pressure treatment from 50 MPa to 150 MPa is not able to ensure better results in terms of density and hardness for both HPT6 and HIP+T6 cycles.

Considering the impact behavior, the positive influence of densification via high-pressure treatments is particularly evident in terms of initiation energy. In fact, if as-cast and HIP samples are considered, after HIP the initiation energy is significantly higher. This is mainly attributed to the low level of porosities, which easily play the role of stress concentration point and, in addition, reduce the load-bearing area. This is further supported by the observation of the fracture surfaces of as-cast and annealed samples, where several porosities were present. Moreover, a positive effect of densification on the peak force can

be assessed. Nevertheless, the highest increase in peak force is achieved when, besides the densification, the Al matrix is strengthened after aging treatments, increasing the yield strength of the alloy (HIP+T6 and HPT6 conditions). In these cases, the fracture initiates mainly due to the cracking or detachment of brittle particles, such as eutectic Si and intermetallic particles. No significant influence of high-pressure treatments on the propagation energy was assessed, with the propagation mainly governed by brittle particles.

FUNDING

Financed by the European Union - NextGenerationEU (National Sustainable Mobility Center CN00000023, Italian Ministry of University and Research Decree n. 1033 - 17/06/2022, Spoke 11 - Innovative Materials & Lightweighting). The opinions expressed are those of the authors only and should not be considered as representative of the European Union or the European Commission's official position. Neither the European Union nor the European Commission can be held responsible for them.

ACKNOWLEDGMENTS

The authors wish to acknowledge:

- Peli F. and Coffetti A. of the Department of Mechanical and Industrial Engineering of the University of Brescia for the support in samples machining.
- Boschini N. of the Department of Engineering of the University of Ferrara for the support in samples testing.
- Cosio D. of Ghial S.p.A. for providing the gravity cast components.
- Shipley J. of Quintus Technologies AB for hot isostatic pressing (HIP and HPT6) treatments.

REFERENCES

[1] Francis, J. A., and Cantin, G. D. (2005). The role of defects in the fracture of an Al–Si–Mg cast alloy, Materials Science and Engineering: A, 407 (1-2), pp. 322–329. DOI: 10.1016/j.msea.2005.07.042

[2] Girelli, L., Tocci, M., Montesano, L., Gelfi, M., and Pola, A. (2018). Investigation of cavitation erosion resistance of AlSi10Mg alloy for additive manufacturing. Wear, 402-403, pp. 124-136. DOI: 10.1016/j.wear/2018.02.018

[3] Liu, X., Liu, Y., Zhou, Z., Zhong, H., & Zhan, Q. (2022). A combination strategy for additive manufacturing of AA2024 high-strength aluminium alloys fabricated by laser powder deb fusion: Role of hot isostatic pressing, Materials Science and Engineering: A, 850, 143597. DOI: 10.1016/j.msea.2022.143597

[4] Girelli, L., Giovagnoli, M., Tocci, M., Pola, A., Fortini, A., Merlin, M., and La Vecchia, G. M. (2019). Evaluation of impact behaviour of AlSi10Mg alloy produced by laser additive manufacturing, Materials Science and Engineering: A, 748, pp. 38-51. DOI: 10.1016/j.msea.2019.01.078

[5] Nyahumwa, C., Green, N. R., and Campbell, J. (2001). Influence of casting technique and hot isostatic pressing on the fatigue of an Al-7Si-Mg alloy, Metallurgical and Materials Transactions A: Physical Metallurgy and Materials Science, 32, pp. 349-358. DOI: 10.1007/s11661-001-0266-8

[6] Staley, J. T., Tiryakioğlu, M., and Campbell, J. (2007). The effect of hot isostatic pressing (HIP) on the fatigue life of A206-T71 aluminum castings, Materials Science and Engineering A, 465 (1-2), pp. 136-145. DOI: 10.1016/j.msea.2007.02.009

[7] Ceschini, L., Morri, A., and Sambogna, G. (2008). The effect of hot isostatic pressing on the fatigue behaviour of sand-cast A356-T6 and A204-T6 aluminum alloys, Journal of Materials Processing Technology, 204 (1-3), pp. 231-238. DOI: 10.1016/j.jmatprotec.2007.11.067

[8] Ceschini, L., Boromei, I., Morri, A., Seifeddine, S., and Svensson, I. L. (2012). Effect of Fe content and microstructural features on the tensile and fatigue properties of the Al–Si10–Cu2 alloy, Materials and Design (1980-2015), 36, pp. 522–528. DOI: 10.1016/jmatdes.2011.11.047

[9] Ran, G., Zhou, J., and Wang, Q. G. (2006). The effect of hot isostatic pressing on the microstructure and tensile properties of an unmodified A356-T6 cast aluminum alloy. Journal of Alloys and Compounds, 421 (1-2), pp. 80-86. DOI: 10.1016/j.jallcom.2005.11.019

[10] Lee, M. H., Kim, J. J., Kim, K. H., Kim, N. J., Lee, S., and Lee, E. W. (2003). Effects of HIPping on high-cycle fatigue properties of investment cast A356 aluminum alloys, Materials Science and Engineering: A, 340 (1-2), pp.123-129. DOI: 10.1016/S0921-5093(02)00157-0

[11] Hafenstein, S., Brummer, M., Ahlfors, M., and Werner, E. (2016). Combined Hot Isostatic Pressing and Heat Treatment of Aluminum A356 Cast Alloys, HTM Journal of Heat Treatment and Materials, 71(3), pp. 117-124. DOI: 10.3139/105.110281

[12] Hafenstein, S., and Werner, E. (2018). Simultaneous hot isostatic pressing and solution annealing of aluminum cast alloys followed by instantaneous aging at elevated temperatures, IOP Conference Series: Materials and Engineering, 416, (012084), 7th International Conference on Advanced Materials and Structures – AMS 2018, Romania, DOI: 10.1088/1757-899X/416/1/012084

[13] Tocci, M., Pola, A., Gelfi, M., and La Vecchia, G. M. (2020). Effect of a New High-Pressure Heat Treatment on Additively Manufactured AlSi10Mg Alloy, Metallurgical and Material Transactions A, 51, pp. 4799-4811. DOI: 10.1007/s11661-020-05905-y

[14] Giovagnoli, M., Tocci, M., Fortini, A., Merlin, M., Ferroni, M., and Pola, A. (2022). On the Anisotropic Impact Behavior of an Additively Manufactured AlSi10Mg Alloy in Different Heat Treatment Conditions, Journal of Materials Engineering and Perfomance, 31, pp. 6806-6818. DOI: 10.1007/s11665-022-06696-6

[15] Taylor, J. A. (2012). Iron-Containing Intermetallic Phases in Al-Si Based Casting Alloys, Procedia Materials Science, 1, pp. 19-33. DOI: 10.1016/j.mspro.2012.06.004

[16] Davis J. R. (1993), ASM Specialty Handbook: Aluminum and Aluminum Alloys, ASM International. ISBN: 978-0-87170-496-2

[17] Lasagni, F., Mohammadian, H. R., Falahati, A., and Desischer, H. P. (2006). Volume change of Si-containing Al-alloys during ageing. 15th Congress IFTHSE (International Federation for Heat Treatment and Surface Engineering and Surface Modification Technologies), Vienna, Austria.

[18] Dighe, M. D., Gokhale Fasm, A. M., and Horstemeyer, M. F. (2002). Effect of loading condition and stress state on damage evolution of silicon particles in an Al-Si-Mg-Base cast alloy, Metallurgical and Materials Transactions A, 33, pp. 555-565. DOI: 10.1007/s11661-002-0117-2

[19] Zhang, D. L., Zheng, L. H, StJohn, D. H, (2002). Effect of a short solution treatment time on microstructure and mechanical properties of modified Al–7wt.%Si–0.3wt.%Mg alloy, Journal of Light Metals, 2(1), pp. 27-36. DOI: 10.1016/S1471-5317(02)00010-X

[20] Merlin, M., Timelli, G., Bonollo, F., Garagnani, G. L., (2009). Impact behaviour of A356 alloy for low-pressure die casting automotive wheels, Journal of Materials Processing Technology, 209(2), pp. 1060-1073, DOI: 10.1016/j.jmatprotec.2008.03.027

[21] Malgorzata, W. Aliminum-Silicon Casting Alloys: Atlas of Microfractographs, ASM International. ISBN: 978-0-87170-794-9